48 *KSME International Journal, Vol. 17 No. 1, pp. 48~56, 2003*

Impact Collapse Characteristics of CF/Epoxy Composite Tubes for Light-Weights

Young Nam Kim, Jae Jung Hwang, Kyung Yun Baek
Department of Mechanical Design Engineering Graduate school, Chosun University, 375 Seosuk-dong, Dong-gu, Kwangju 501-759, Korea
Cheon Seok Cha
Division of Aerospace and Naval Architectural Engineering, Chosun Univeristy, 375 Seosuk-dong, Dong-gu, Kwangju 501-759, Korea
In Young Yang*
School of Mechanical Engineering, Chosun University, 375 Seosuk-dong, Dong-gu, Kwangju 501-759, Korea

This paper investigates the collapse characteristics of CF/Epoxy composite tubes subjected to axial loads as changing interlaminar number and outer ply orientation angle. The tubes are aften used for automobiles, aerospace vehicles, trains, ships, and elevators. We have performed static and dynamic impact collapse tests by a way of building impact test machine with vertical air-compression. It is fanad that CF/Epoxy tube of the 6 interlaminar number (C-type) with 90° outer orientation angle and trigger absorbed more energy than the other tubes (A, B and D-types). Also collapse mode depended upon outer orientation angle of CF/Epoxy tubes and loading type as well; typical collapse modes of CF/Epoxy tubes are wedged, splayed and fragmentcl.

Key Words: CF/Epoxy Composite Tube, Impact Collapse Characteristics, Interlaminar Number, Outer Ply Orientation Angle, Trigger, Wedge Collapse Mode, Splaying Collapse Mode, Fragmentation Collapse Mode

1. Introduction

Because of their high strength, stiffness to density, composites are considered for many structural applications such as aerospace vehicles, automobiles, trains and ships. Composite materials exhibit collapse modes that are significantly different from the crushing modes of metallic materials, and composite materials are efficient energy absorbing materials (Gupta et al., 1997).

So for many studies have been conducted to study the effect of reinforcement, crush rate, environment temperature, and specimen architecture on the energy absorption of composite tubes. Thornton and Edwards (1982) carried out experiments on the crushing behavior of composite tubes and studied the influence of various parameters on their crushing characteristics. Earlser Thornton (1979) studied the behavior of FRP tubes of glass, graphite and Kevlar fiber reinforced epoxy resin with different lay-up and t/D ratio, and showed that the specific energy absorption of FRP tubes exceeds that of the high strength metallic tubes. In experiments Thornton introduced the 45° bevel at one end of tube to initiate the deformation at the end, irrespective of the fiber orientation and lay-up in the tube. It was reported as results that all the tubes collapsed by disintegration except the [45/-45] Kevlar/

* Corresponding Author,
E-mail : iyyang@mail.chosun.ac.kr
TEL : +82-62-230-7169; **FAX** : +82-62-230-7170
School of Mechanical Engineering, Chosun University, 375 Seosuk-dong, Dong-gu, Kwangju 501-759, Korea.
(Manuscript **Received** March 2, 2001; **Revised** November 5, 2002)

epoxy tubes, which did by buckling like metal tubes. Moreover the specific energy of the tubes was found to be less sensitive to the t/D ratio than that of metal tubes. Thornton also conducted experiments on Kevlar, graphite, and glass fiber, reinforced epoxy resin tubes of rectangular, square and round cross section, and observed that tubes of planar section were less effective at energy absorption than those of circular section.

Farley and Jones (1991) studied the effect of crushing speed on the energy absorbing characteristics of Kevlar/epoxy tubes, and found that their specific energy at $[0/\pm\theta]$ fiber orientations did not vary with crushing speed, whereas in tubes of $[\pm\theta]$ fiber orientations, it increased with crushing speed. The angles of fiber orientation in their experiments were 45° to 75°. In Kevlar/epoxy tubes, however, the energy absorbing capacity increased with speed in all cases of consideration. Farley and Jones carried out further analytical studies to determine the specific sustained energy for different ply orientation and geometry of Kevlar/epoxy and graphite/epoxy tubes. A commercially available FEM package was used for this purpose.

Farley and Jones (1992) also identified three unique crushing modes which occur in continuous-fiber reinforced composite tubes, namely transverse shearing, lamina bending and local buckling, as depicted in Fig 1. Most composite materials reinforced with brittle fibers crush in a combination of the transverse shearing and lamina bending modes referred to as the brittle fracturing crushing mode. Fair full and Hull (1989) carried out experiments to study the frictional energy involved in the crushing of composite tubes between plates with different roughness, and identified to classify different factors that contribute to the energy dissipation of tubes.

Previous studies on the collapse characteristics of composite tubes have involved only collapse testing and determined of the effects of shap as t/D ratio and fiber orientation. The objective of this study was to determine, in CF/Epoxy(Carbon Fiber/Epoxy Resin) composite tubes, the interlaminar number and outer ply orientation angles affecting the crushing characterestics and energy absorption capability and to advance the fundamental understanding of collapse mechanism and modes of composite tubes under impact loading.

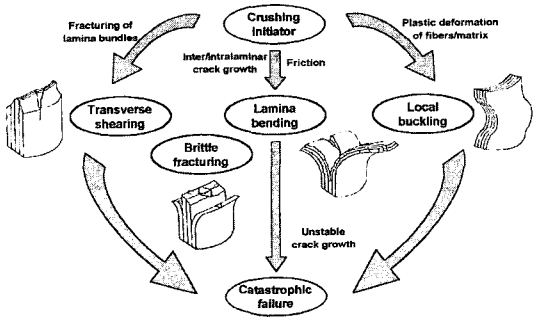

Fig. 1 Crushing process of continuous fiber reinfroced composite tubes (Farley and Jones, 1992)

2. Specimens

CF/Epoxy composite tubes were manufactured from the unidirectional prepreg sheets of carbon fibers (CU125NS) by the HANKUK Fiber Co. in Korea. The CF/Epoxy tubes were made of 8 layers of these sheets stacked at different angles. The ply cured of the tape prepreg was 0.125 mm in thickness. Prepreg material was wrapped around a metal mandrel using a table wrapper. Specimens were heat cured to the appropriate hardening temperature (130℃) as a heater at the vacuum bag of an autoclave. Tubes, of 30 mm inside diameter, were cut into 100 mm length by a diamond cutting machine. One end of each tube was then chamfered at 45° so that crushing may

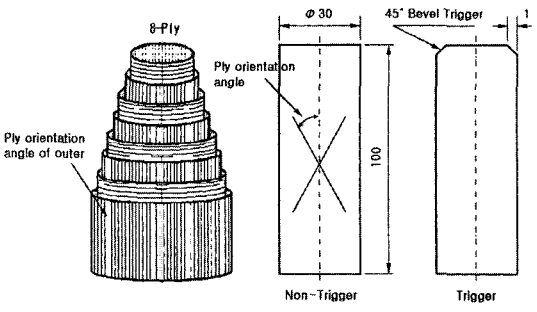

Fig. 2 The shapes of specimen (unit : mm)

Table 1 Material properties of the specimen

Characteristics \ Types	Fiber (Carbon)	Resin (Epoxy #2500)	Prepreg Sheet (CU125NS)
Density [kg/m³]	1.83×10^3	1.24×10^3	–
Tensile Strength [GPa]	4.89	0.08	2.53
Elastic Modulus [GPa]	240	3.50	138
Breaking Elongation [%]	2.1	3.0	1.7
Poisson's ratio	–	–	0.30
Resin Content	–	–	37[% wt]
Curing Temperature	–	130℃	130℃×90min

Table 2 Specimen designation

S(I) A(B, C, D) 00(90) T(N)

- Load
  - S : Static
  - I : Impact
- Interlaminar number(I.N.)
  - A : $[0_2/90_2]_S$ or $[90_2/0_2]_S$(I.N.=2)
  - B : $[90_2/0_2]_2$ or $[0_2/90_2]_2$(I.N.=3)
  - C : $[0/90]_{2S}$ or $[90/0]_{2S}$(I.N.=5)
  - D : $[90/0]_4$ or $[0/90]_4$(I.N.=7)
- Outer ply orientation angle
  - 00 : Orientation angle of outer is 0°
  - 90 : Orientation angle of outer is 90°
- Trigger/Non-trigger
  - T : Trigger
  - N : Non-Trigger(without trigger)

be initiated without causing catastrophic failure as in Fig. 2. Table 1 lists the material properties of the specimen and Table 2 designates the specimen. In Table 2, A is the interlaminar number= 2, B is 3, C is 6 and D is 7. The outer ply orientation angle is 90° in the case of layer-ups for the under line stacking method, and 0° in the case of layer-ups for the other. Their marks are to 90 and 00. Also, specimens with trigger are labelled T and those without trigger are labelled N.

3. Apparatus and Experiment

3.1 Axial static collapse test

The static axial collapse test was performed to examine with changing the interlaminar number, outer ply orientation angle and trigger, by a universal test machine of 5 ton capacity. Loading

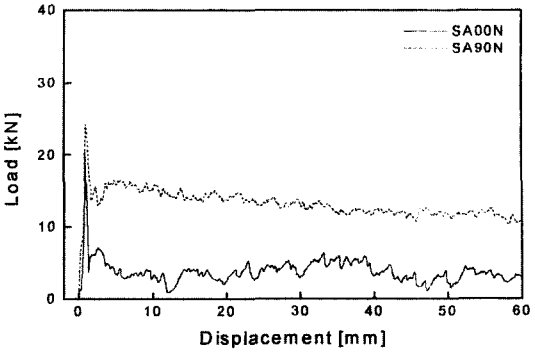

Fig. 3 Relationship between load and displacement, SA_N

plates were set parallel to each other prior to the initiation of tests. Load-displacement curve was recorded by an compositeized data acquisition system. In case of the static compression test, all tubes were guasi-statically compressed at a rate of 10mm/min. until the displacement of 60 mm was reached. Each test was repeated at least three times and in some cases done four or five times. The absorbed energy is repesented by the area of the load-displacement curve as shown in Fig. 3 and thus obtained by integrating the load against displacement as shown by Eq. (1), and the average collapse load is calculated by dividing the absorbed energy by the deformed length. The average collapse stress is then calculated by dividing the average collapse load by the sectional area of specimen, as shown by Eq. (2).

$$E_a=\int Pdl \tag{1}$$

$$\sigma_{av}=\frac{P_{av}}{A}=\frac{E_a/\delta}{2\pi Rt} \tag{2}$$

where E_a is the absorbed energy in the specimen, P is the collapse load during the crushing process, σ_{av} is the average collapse stress, P_{av} is the average collapse load, and δ is the deformed length.

Figure 3 is the load-displacement curve of the static test on the CF/Epoxy composite tubes. The solid line represents the 0° outer ply orientation angle with the interlaminar number of 2 and the broken line represents the 90° outer ply orientation angle of the same interlaminar number. Figures 4 and 5 show collapse process of CF/

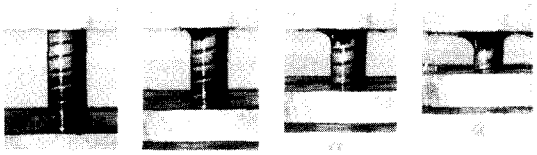

Fig. 4 Collapse process of CF/Epoxy composite tubes with a 0° outer ply orientation angle, SA00N

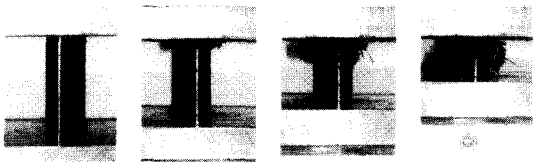

Fig. 5 Collapse process of CF/Epoxy composite tubes with a 90° outer ply orientation angle, SA90N

(a) SA00N (b) SA90N

Fig. 6 Collapsed shape of composite tubes without trigger after static testing

Epoxy composite tubes, and Fig. 5 shows the collapsed shape under static load. Figure 6(a) shows a specimen with a 0° outer ply orientation angle and Fig. 6(b) shows a 90° outer ply orientation angle.

3.2 Axial impact collapse test

Axial impact collapse tests were performed by using a vertical impact testing machine and load cell. The vertical impact testing machine is shown in Fig 7. The cross head, which is accelerated by compressed air, collides with specimens on the load cell. The cross head weight was 40 kg. The impact velocity was measured by a laser system before the cross head collided with the specimen. The value of the impact energy is 783 J at 6.26 m/sec, which is similar to that obtained by using Eq. (3).

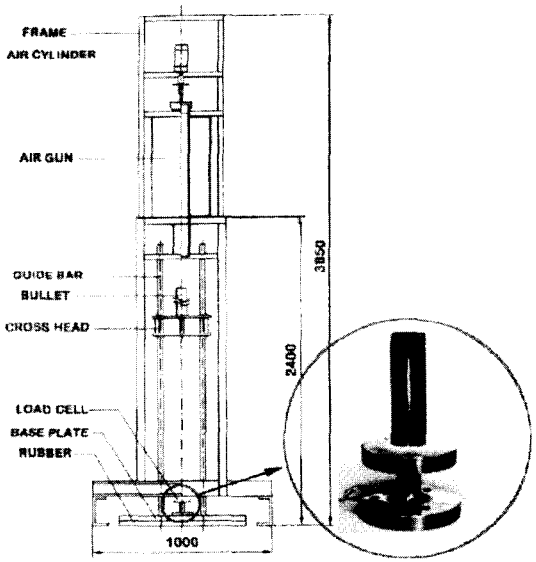

Fig. 7 The vertical impact testing machine

$$E_I=\frac{1}{2}mv^2 \tag{3}$$

where m is the mass of the cross head and v (6.26 m/sec) is the impact collapse velocity.

The load cell has two mild steel circular plates connected by a cylindrical column. Specimens are placed on the upper plate. The lower plate has three holes for fixing on the base. Two semiconductor strain gauges (KYOWA, KSP-2-120 E4) are symmetrically placed on both sides of the load cell. Series connection was used between the two gauges to eliminate the bending effect. During the test, impact loads were obtained by converting electrical resistance variations on the semiconductor strain gauge into loads. The resistance variations of the semiconductor strain gauge with the shield line and the bridge box are fed into a dynamic strain amplifier which converts them into voltage variations. Deformation of a specimen is measured by using a non-contacting optical deformation system (ZIMMER 100F), which catches the movement of the target on the cross head.

A load-deformation curve showing the collapse history is obtained by eliminating the time axis from each measured time-load and time-deformation curve. Based on the load-deformation curve, absorbed energy (E_a), average col-

lapse load (P_{av}), average collapse stress (σ_{av}) and maximum collapse load (P_{max}) are derived. The energy absorption characteristics and collapse modes of each specimens may then be investigated. Figure 8 represents the load-deformation diagram of a specimen with the interlaminar number of 2 after impact testing. The solid line is of the 0° outer ply orientation angle and the broken line is of the 90° outer ply orientation angle. Figure 9 presents collapsed specimen shapes.

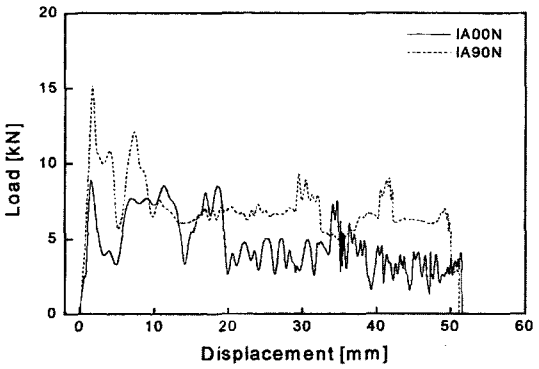

Fig. 8 Relationship between load and displacement, IA_N

(a) IA00N (b) IA90N

Fig. 9 Collapsed shape of the composite tube without trigger after impact testing

4. Results and Discussion

4.1 The collapse characteristics of composite tubes

An experimental investigation was conducted to determine whether the energy absorption capability of the circular composite tubes is a function of interlaminar number, outer ply orientation angle and trigger, Absorbed energy E_a, average collapse load P_{av}, maximum load P_{max} and average collapse stress σ_{av} were derived and collapse modes considered in terms of there variables, interlaminar number, outer ply orientation angle and the trigger. Results varied significantly as a function of the ply orientation angle, the interlaminar number and trigger.

Figures. 10~13 compare the mean values of the maximum loads and the average collapse stresses of the static and impact collapse tests by changing interlaminar number, outer ply orientation angle and trigger/non-trigger. The maximum load is shown in Fig. 10. In static tests, the maximum collapse load of composite tubes without a trigger increases as the interlaminar number increases as shown in Fig. 10(a), but those with a trigger produced a constant level with increasing interlaminar number as shown in Fig. 10(b). This is

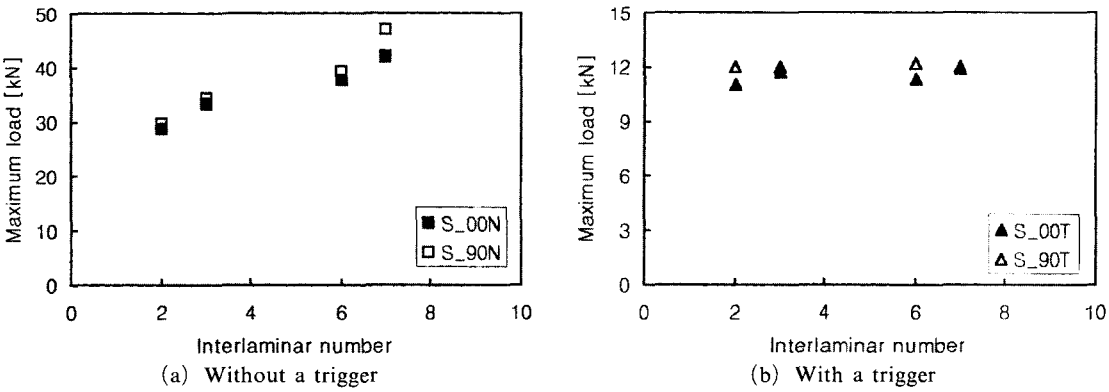

(a) Without a trigger (b) With a trigger

Fig. 10 Relationship between the maximum load and the interlaminar number for various CF/Epoxy thin-wall structures under static load

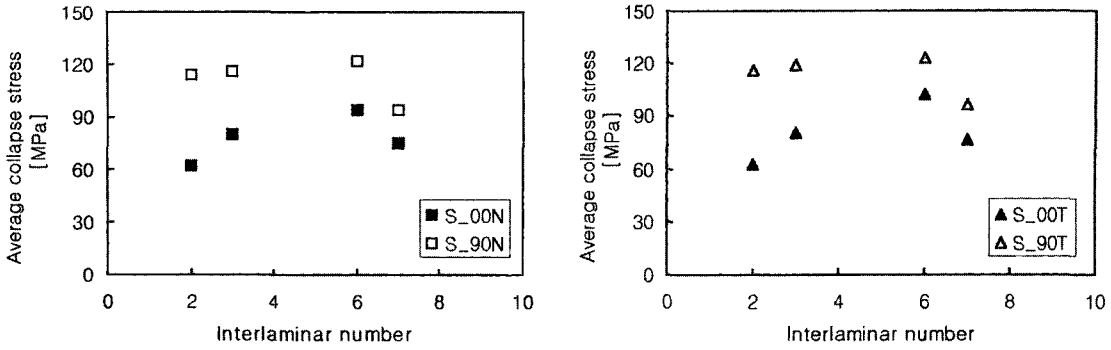

(a) Without a trigger (b) With a trigger

Fig. 11 Relationship between the average collapse stress and the interlaminar number for various CF/Epoxy thin-wall structures under static load

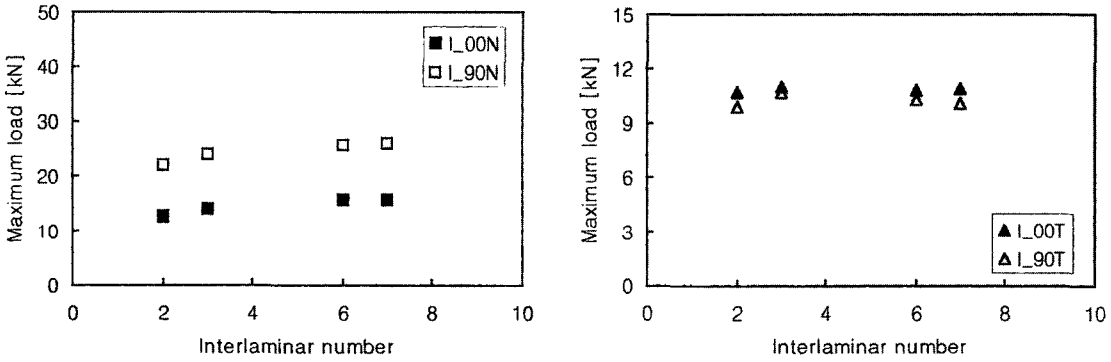

(a) Without a trigger (b) With a trigger

Fig. 12 Relationship between the maximum load and the interlaminar number for various CF/Epoxy thin-wall structures under impact load

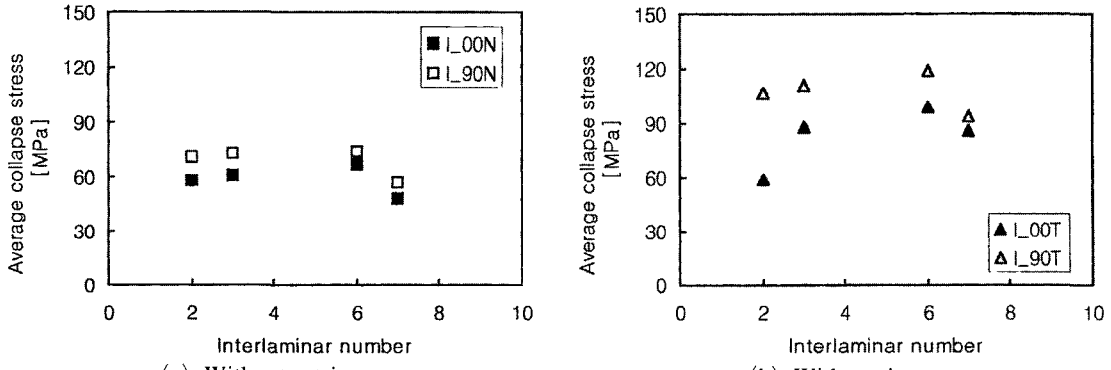

(a) Without a trigger (b) With a trigger

Fig. 13 Relationship between the average collapse stress and the interlaminar number for various CF/Epoxy thin-wall structures under impact load

because the trigger becomes the initial failure of the composite tubes during loading. Therefore the maximum load of composite tubes with trigger is lower, but the average collapse stress does not follow same trend as the maximum collapse load.

The average collapse stress is presented in Fig. 11, showing that the average collapse stress increases to the interlaminar number of 6, with

increasing interlaminar number. However, decreasing trend is observed on moving to the interlaminar number of 7. Since a key element of the energy absorption is the crack growth and extension, the cracks may be classified as interlaminar cracks, intralaminar cracks and central cracks. It is apparent that the interlaminar cracks increase, but the growth of intralaminar and central cracks decrease with increasing interlaminar number. Also in case of a C-type stacking with the interlaminar number of 6, the CF/Epoxy composite tube is stacked symmetrically about the center of the tube, but not symmetrically in the case of a D-type with the interlaminar number of 7. The maximum collapse load and average collapse stress under impact tests show the same trend as the static tests, as shown in Figs. 12 and 13.

In all tests, CF/Epoxy composite tubes with a 90° outer ply orientation angle exhibit a higher crush load throughout the whole crush process and the average collapse stress of composite tubes with a 90° outer ply orientation angle is higher than those with a 0° outer ply orientation angle because the outer-fibers extend and break.

4.1 The collapse mode of composite tubes

The collapse mode depended on the outer ply orientation angle and the loading type (static/impact). The collapse modes of the CF/Epoxy composite tube are three: the wedge collapse mode, the splaying collapse mode, and the fragmentation collapse mode. The wedge collapse mode was shown in case of the CF/Epoxy composite tubes with a 0° outer ply orientation angle under static and impact loading. The splaying collapse mode was shown only in the case of tubes with a 90° outer ply orientation angle under static loading, whereas those were collapsed in a fragmentation mode during the impact testing.

Figure 14 is a section of a CF/Epoxy composite tube showing the wedge collapse mode. A photograph of a typical section through the collapse zone of a CF/Epoxy composite tube is shown in Fig. 15. Three unique crushing modes, as defined by Farley and Jones (1992) are exhibited by continuous fiber-reinforced composite

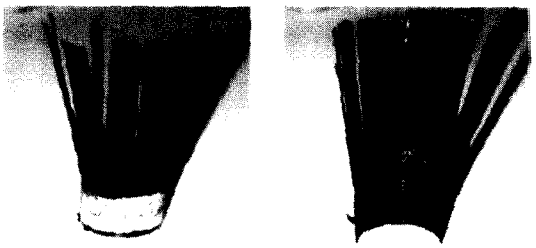

Fig. 14 Section of composite tube showing the wedge collapse mode, SA00N

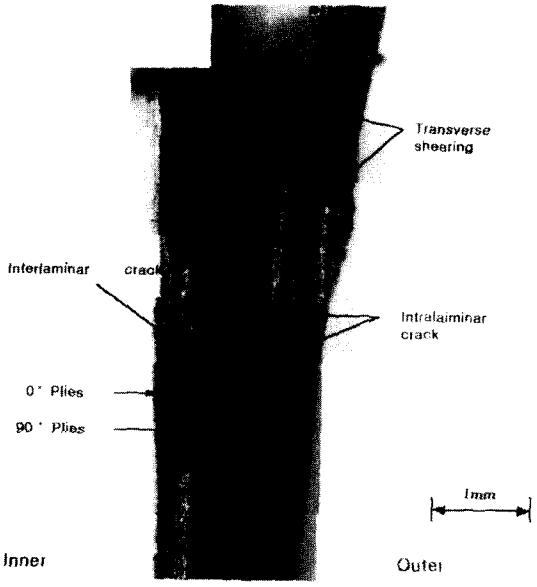

Fig. 15 Photomicrograph of a section through the crush zone of CF/Epoxy composite tube showing wedge collapse mode

tubes as transverse shearing, lamina bending and local buckling. Most tubes fabricated from brittle fiber reinforcement crush in a combination of transverse shearing and lamina bending modes. This combined crushing mode is referred to as the brittle fracturing collapse. Figures. 14 and 15 show the basic collapse mode of brittle fiber reinforced composite tubes, which is described as the fracture collapse mode. The left of tile photograph is the inner and outer is on the right of Fig. 15. In Fig. 15, the white part is the stacked plies for 0° plies orientation and the black part is the plies for 90° orientation. Fiber and matrix of the 0° plies of the inner and the 90° plies of the center are fractured by bending. The 0° plies of

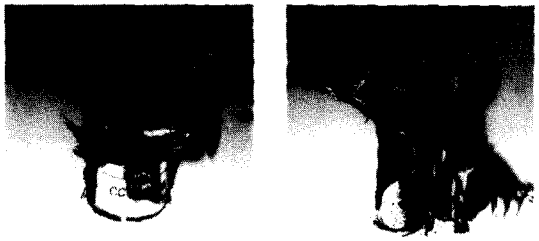

Fig. 16 Section of composite tube showing the splaying collapse mode, SC90N

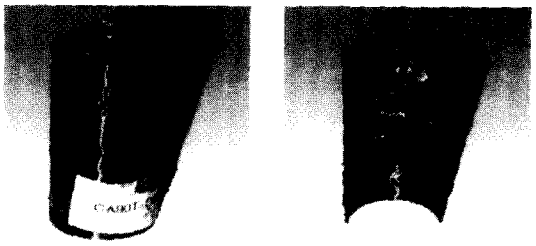

Fig. 18 Section of composite tube showing the fragmentation collapse mode, IA90T

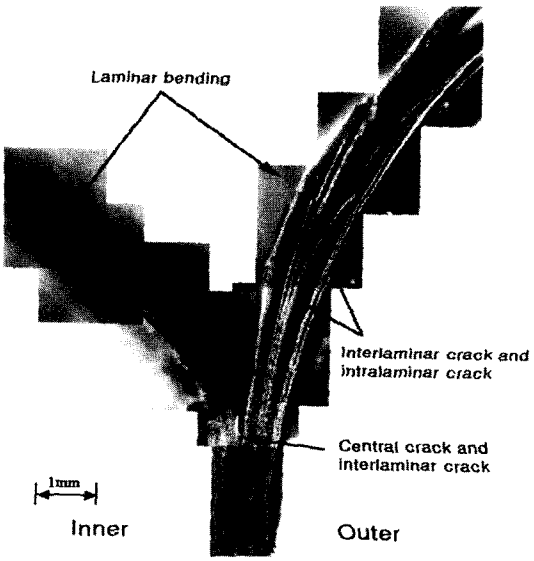

Fig. 17 Photomicrograph of a section through the crush zone of CF/Epoxy composite tube showing splaying collapse mode

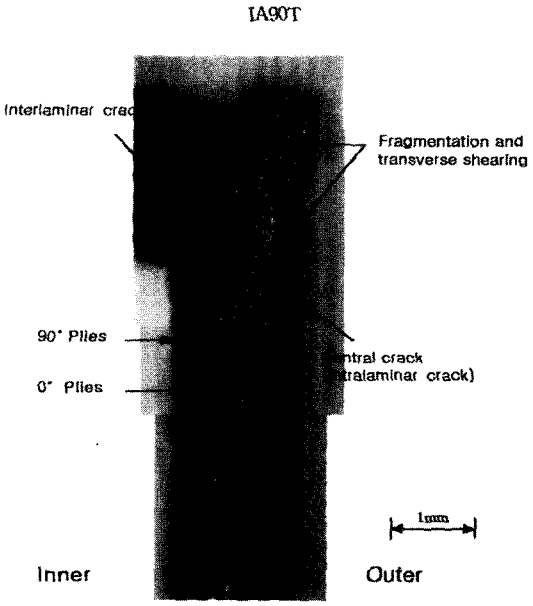

Fig. 19 Photomicrograph of a section through the crush zone of CF/Epoxy composite tube showing fragmentation collapse mode

the outer absorbed the energy by bending but did not fracture. The principal energy-absorption mechanism in the collapse of CF/Epoxy composite tubes is inter/intralaminar crack growth.

Figure 16 is a section of a CF/Epoxy composite tube showing the splaying collapse mode and a photograph of a typical section is shown in Fig. 17. As shown in Figs. 16 and 17, this collapse mode involves the growth of central cracks, inter/intralaminar cracking, and laminar bending.

Figure 18 also shows a section of a CF/Epoxy composite tube that has suffered fragmentation collapse, a photograph of a typical section is shown in Fig. 19. As shown in Figs. 18 and 19, the fiber and matrix of all plies of the inner, outer and center are fractured/sheared, and debris are scattered. Therefore in static tests composite tubes with a 90° outer ply orientation angle is higher than composite tubes with a 0_o outer ply orientation angle because the fibers in the outer laminate tend to extend and break.

5. Conclusion

In this study, CF/Epoxy composite tubes with a variety of interlaminar numbers, outer ply orientation angles and trigger are presented. The results are as follows:

(1) In all tests, the maximum collapse load of the composite tubes without a trigger increased as the interlaminar number increased, and those

with a trigger produced almost same values.

(2) CF/Epoxy composite tubes with a 90° outer ply orientation angle exhibited higher crush loads throughout the whole crush increases, and the higher energy absorption capability (average collapse load and average collapse stress) of the composite tubes with a 90° outer ply orientation angle is higher than those of tubes with a 0° outer ply orientation angle because in this case the outer-fiber extend and break.

(3) In the case of the collapse of the brittle fiber reinforced composite tube, the collapse mode depended upon the outer ply orientation angle and the loading type (static/impact). The wedge collapse mode was shown by CF/Epoxy composite tubes with a 0° outer ply orientation angle under static and impact loading. The splaying collapse mode was shown only by tubes with a 90° outer ply orientation angle under static loading, whereas these collapsed by the fragmentation mode during impact testing.

(4) The energy absorption capability of all CF/Epoxy composite tubes was determined to be a function of the interlaminar number, the outer ply orientation angle and upon the presence of a trigger. Higher energy absorbtion occurred for composite tubes with the interlaminar number of 6, a 90° outer ply orientation angle and a trigger.

Acknowledgment

This work was supported by Korea Research Foundation Grant. (KRF-2001-041-E00055)

References

Fairfull, A. H. and Hull, D., 1989, "Energy Absorption of Polymer Matrix Composite Structures : Frictional Effects," *In : Structural Failure, Edted. by T. Wierzbicki and N. Jones, New York : Willey*, pp. 255~279.

Farley, G. L. and Jones, R. M., 1991, "The Effects of Crushing Speed on the Energy-Absorption Capability of Composite Tubes," *Journal of Composite Materials*, Vol. 25, pp. 1314~1329.

Farley, G. L. and Jones, R. M., 1992, "Crushing Characteristics of Continuous Fiber-Reinforced Composite Tubes," *Journal of Composite Materials*, Vol. 25(1), pp. 37~50

Farley, G. L. and Jones, R. M., 1992. "Prediction of the Energy-Absorption Capability of Composite Tubes," *Journal of Composite Materials*, Vol. 25(3), pp. 388~404.

Gupta, N. K., Velmurugan, R. and Gupta, S. K., 1997, "An Analysis of Axial Crushing of Composite Tubes," *Journal of Composite Materials*, Vol. 31, pp. 1252~1285.

Hamada, H., Ramakrishna, S., Nakamura, M. and Maekawa., Z., 1994, "Comparison of Static and Impact Energy Absorption of Glass Cloth/Epoxy Composite Tubes," *Proceedings of the 10th Annual ASM/ESD Advanced Composite Conference*, pp. 501~510.

Kim, Y. N., Choi, H. S., Cha, C. S., Im, K. H., Jung, J. A. and Yang, I. Y., 2000, "Influence of Stacking Sequence Conditions on the Characteristics of Impact Collapse using CFRP Thin-Wall Structures," *KSME Journal A*, Vol. 24, No. 12, pp. 2945~2951.

Kim, Y. N., Im, K. H., Park, J. W. and Yang, I. Y., 2000, "Experimental Approach on the Colapse Mechanism of CFRP Composite Tubes," *Rewiews of Progress in QNDE*, pp. 359~375.

Tashiro, S., Yokoyama, A. and Hamada, H., 1998, "Numerical Method of Impact Deformation and Failure in Composite Tubes," *JSMS Composites-27*, pp. 297~298.

Thornton, P. H. and Edwards, P. J., 1982, "Energy Absorption in Composite Tubes," *Journal of Composite Materials*, Vol. 15, pp. 521~545.

Thornton, P. H., 1979, "Energy Absorption in Composite Structrues," *Journal of Composite Materials*, Vol. 13, pp. 247~253.